KSABC
The Korean Society for Applied Biological Chemistry

ARTICLE

Open Access

Therapeutic effects of TMF and catechol in pulmonary fibrosis: in vitro and in vivo analysis

Jin-Hyuk Choi[1], Youngmee Kim[1,2,3*] and Moonjae Cho[1,2*]

Abstract

Idiopathic pulmonary fibrosis is a fatal lung disorder characterized by abnormal deposition of extracellular matrix (ECM), which is secreted by activated myofibroblasts. While the origin of myofibroblasts has been discussed, epithelial-mesenchymal transition (EMT) is being noticed as one of the mechanisms of myofibroblast activation. Recent studies have shown that reactive oxygen species appear to induce not only EMT but also fibrotic progression and maintenance. Therefore, we tested chemicals that have antioxidant capacity as drugs for fibrosis. To evaluate the effects of 4′,6,7-trimethoxyisoflavone (TMF) and catechol (CAT) on EMT and fibrosis, we used an in vitro transforming growth factor (TGF)-β1 or bleomycin-induced model and an in vivo BLM-induced model. The results showed that the co-administration of TMF/CAT ameliorated pulmonary fibrosis by decreasing EMT and ECM accumulation by hindering both Smad and non-Smad TGF-β signalling cascades. Furthermore, significant increases in the number of total immune cells (especially lymphocytes) were observed in BLM-treated animals treated with TMF/CAT. Our findings suggest that co-intervention with TMF/CAT may be a potential treatment for fibrosis.

Keywords Catechol, Pulmonary fibrosis, ROS, TMF

Introduction

Fibrosis is a serious medical condition that can affect any organ. It is responsible for up to 45% of all fatalities in industrialized nations. Fibrosis, on the other hand, is not a disease but rather an usual pathological result of the dysregulated wound healing process [1]. The wound healing response initiates when local fibroblasts are stimulated and increase their secretion of growth factors, inflammatory cytokines, and extracellular matrix (ECM) components [2, 3]. Wound healing is effective when the damage is small or non-repetitive, leading to only a temporary increase in the accumulation of ECM components and restoration of functional tissue architecture. Normal tissue repair can develop into a gradual irreversible fibrotic response if tissue injury is severe or persistent [3]. This response, known as fibrosis, is characterized by an excessive accumulation of ECM proteins (such as fibronectin and collagen) in and around inflamed or damaged tissue. Representative fibrotic outcomes include idiopathic pulmonary fibrosis (IPF), end-stage liver disease, kidney disease, and heart failure. [4].

The prevalence of IPF, the most often diagnosed interstitial lung disorders, is rising globally [5]. IPF is a very severe condition in which clinical decline is frequent, despite the fact that the novel antifibrotic drugs pirfenidone and nintedanib reduce the progressive decrease in lung function [6]. Considering the severity and mortality rate of IPF, advanced research needs to be conducted. Even while our knowledge of the pathophysiology of

*Correspondence:
Youngmee Kim
Moonjae Cho
moonjcho@jejunu.ac.kr
[1] Department of Biochemistry, School of Medicine, Jeju National University, Jeju-Si 63241, Korea
[2] Department of Biochemistry, School of Medicine, Institute of Medical Science, Jeju National University, Jeju-Si 63241, Korea
[3] Achem bio, Jeju, Korea

Springer Open

Choi *et al. Applied Biological Chemistry*   (2023) 66:9

Page 2 of 15

fibrosis has considerably increased recently, much of its mechanism is still unclear.

Recent studies suggest that oxidative stress, in which the balance between the production of reactive oxygen species (ROS) and their breakdown by the antioxidant system is changed in favor of a pro-oxidant state, is one of the mechanisms that could be prospective therapeutic targets [7, 8]. ROS, also as one of metabolites induced by fibrotic process, can be released from activated fibroblasts and immune cells, along with chemokines and growth factors. Growing data suggests that the production of several growth factors and cytokines are closely related to ROS generation and oxidative stress; hence, feed-forward and feed-back cycles appear to exist [8]. Continuously activated myofibroblasts are vital players in fibrosis, which secrete growth factors and cytokines, in addition to copious amounts of ECM. These profibrotic myofibroblasts in a variety of tissues, can arise from stem cell progenitors which are from epithelial-mesenchymal transition (EMT) or endothelial-mesenchymal transition. Amounting research evidence suggests that increased ROS may stimulate EMT as well as fibroblast migration, proliferation, and differentiation [8, 9].

Finding new antioxidants has received a lot of attention because ROS is implicated in the pathogenesis of other chronic diseases besides fibrosis, such as cancer, cardiovascular, and neurological diseases [10]. Flavonoids (Fig. 1A) are a class of secondary plant phenolics, and their significant antioxidant properties are gaining attention. The structures of flavonoids and isoflavones vary, and they have a variety of health-promoting properties, such as anti-inflammatory, anti-allergic, hepatoprotective, antithrombotic, and antiviral activities [11, 12]. Numerous research have examined the ability of flavonoids to function as antioxidants in vitro, and significant structure–activity relationships have been identified [13]. Comparison of the radical-scavenging efficiency of a series of flavonoids indicated that the ortho-dihydroxy (catechol, CAT) structure (Fig. 1C) in ring B of flavonoids is important for their antioxidant potential [14, 15]. A number of following research carried out in various systems have confirmed the positive effect of CAT in improving the radical scavenging activity of flavonoids and other phenolics [16]. In our previous studies, 4′,6,7-trimethoxyisoflavone (TMF, Fig. 1B), an artificially modified form of an amphiisoflavone isolated from the roots of Amphimas pterocarpoides, was found to affect the interaction between keratinocytes and fibroblasts,

promoting epidermal regeneration and dermal activation [17]. Therefore, we selected TMF and CAT, which have received the most attention among the antioxidant pharmacophores, to test their antifibrotic effects against pulmonary fibrosis.

Herein we studied whether TMF and CAT alone or their co-treatment had any effect in decreasing expression level of mesenchymal cell specific markers and fibrotic proteins, using in vitro transforming growth factor (TGF)-β1 or bleomycin (BLM)-induced experiments and in vivo BLM-induced pulmonary fibrosis models. Changes in the level of inflammatory cytokines were also investigated in vivo.

Materials and methods
Materials
We purchased TMF and CAT from Indofine Chemical Co. (Hillsborough, NJ, USA). High-performance liquid chromatography was utilized to assess their purity and then these were used without further purification. Dimethyl sulfoxide was used to dissolve TMF and CAT. We purchased TGF-β1 from Invitrogen (Waltham, MA, USA) and it was dissolved in $1 \times$ phosphate-buffered saline (PBS). BLM sulfate (mixture) was bought in bulk from Tokyo Chemical Industry Co., Ltd. in Japan (CAS No. 9041934). A stock solution of 20 mg/mL in $1 \times$ PBS was used.

Cell culture
In Dulbecco's modified Eagle's medium (DMEM; Gibco, Waltham, MA, USA), which also contained 10% fetal bovine serum (FBS; Atlas, CO, USA) and 1% $100 \times$ penicillin/streptomycin (P/S) solution (Gibco, Waltham, MA, USA), A549 human alveolar epithelial cells were cultivated. The amount of FBS in DMEM was decreased to 2% during TGF-β1 or BLM treatment of the cells.

MTT assay
Cell viability and cytotoxicity was determined using 3-(4,5-dimethyl-2-thiazolyl)-2,5-diphenyl-2H-tetrazolium bromide (MTT) assay. At a density of 8000 cells per well, cells were seeded into 96-well culture plates before being subjected to varied TMF and CAT concentrations. The experiment was carried out by adding 10 µL of MTT (Sigma-Aldrich, St. Louis, MO, USA) solution (5 mg/mL in PBS) to each well and incubating for 4 h. A spectrophotometer (562 nm) was used to measure the formation of

(See figure on next page.)
Fig. 1 Various concentrations of TMF and CAT do not damage the cell viability. **A** The basic structure of flavonoids. The capacity of radical scavenging of flavonoid tends to increase when it has the CAT structure in its B ring. **B** The structure of TMF. **C** The structure of CAT. **D** For the A549 cell line, TMF and CAT were treated at concentrations of 5 to 40 µM and 0.5 to 5 µM, respectively, and for the co-treatment, 5/0.25, 5/0.5, 10/0.25 and 10/0.5 µM of TMF/CAT was used. All the treatment groups, except the control group, contained the same amount of DMSO which was used to dissolve TMF and CAT. **E** For other types of cell lines, such as myoblast (C2C12) and fibroblasts (HDF, MRC-5), 10 and 0.5 µM for single treatment of TMF and CAT, respectively, was administered or 10/0.5 µM for co-treatment of TMF/CAT
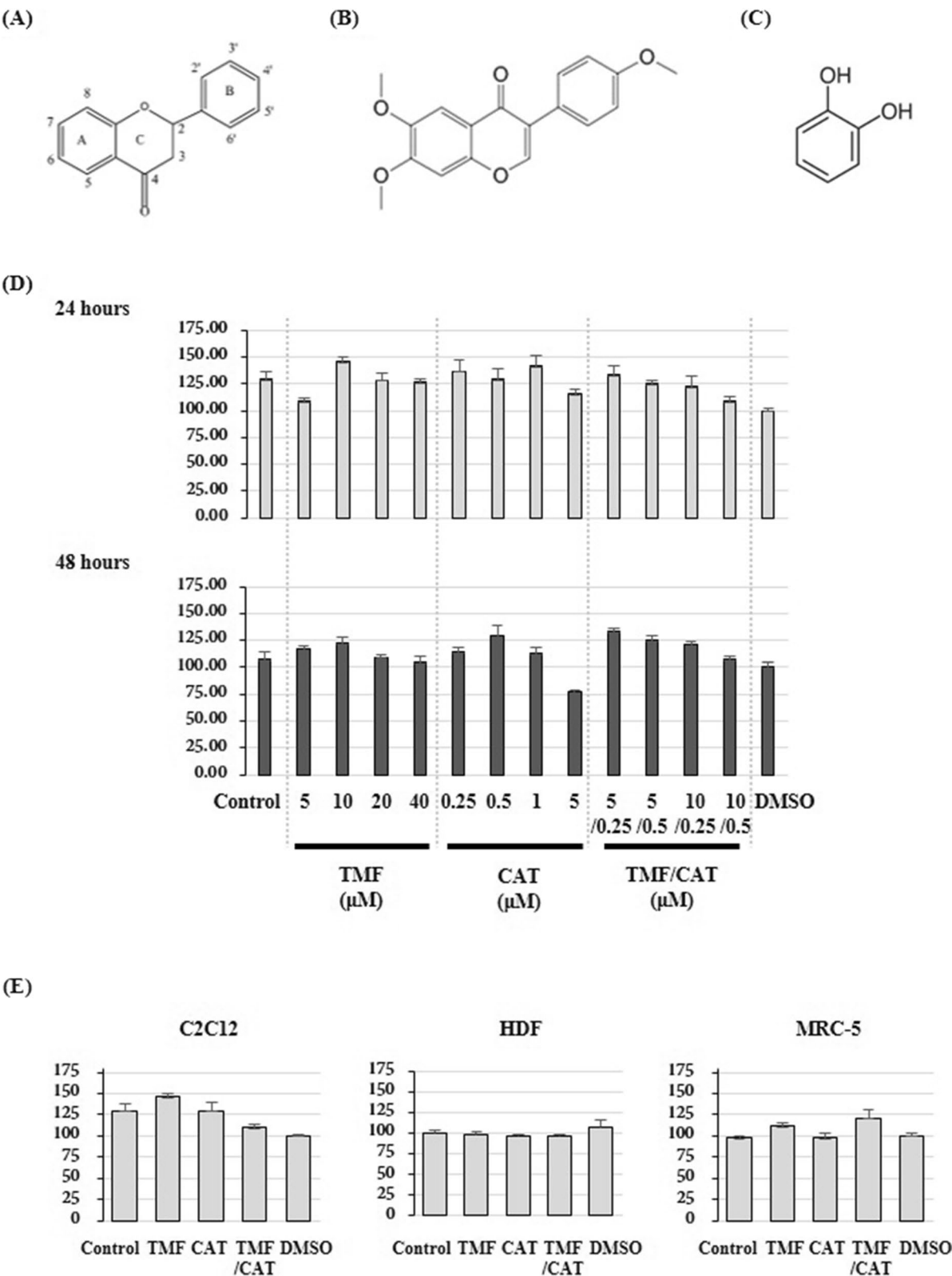
Choi *et al. Applied Biological Chemistry*   (2023) 66:9

Page 3 of 15

Fig. 1 (See legend on previous page.)

formazan crystals after the crystals were dissolved in 200 μL of dimethyl sulfoxide.

Western blot

RIPA buffer was used to extract proteins from the treated cells, and the SMART™ BCA Protein Assay Kit was used to measure them (iNtRON Biotechnology, Gyeonggi-do, Republic of Korea). Equal amounts of each protein sample were loaded into sodium dodecyl sulfate–polyacrylamide gel electrophoresis (SDS-PAGE) and then transferred to a 0.45 μm nitrocellulose blotting membrane. After the blocking using 5% skim milk (made in 1X Tween 20-Tris buffered saline), the membranes were incubated with primary and secondary antibodies followed by four cycles of 10 min washing. The Western ECL kit (LPS Solution, Daejeon, Republic of Korea) was used to detect bands, and ImageJ software was used to quantify them (Bethesda, MD, USA). We used primary antibodies against Fibronectin, Actin, pERK, NOX1, NOX2, NOX4, GAPDH, pP38MAPK, TGF-β1 (Santa Cruz Biotechnology, Dallas, TX. USA), pSMAD2/3, E-cadherin, vimentin, pAKT (Cell Signaling Technology, Beverly, MA, USA), and alpha smooth muscle actin (Sigma-Aldrich, St. Louis, MO, USA). Secondary antibodies (rabbit and mouse) were procured from Koma Biotech (Seoul, Republic of Korea).

Immunofluorescence

The cells were seeded on Lab Tek eight-well chamber slides with a density of 2×10^5 cells/well, fixed with 4% paraformaldehyde in PBS and then washed thrice by PBS. The fixed cells were permeabilized with 0.3% Triton X-100 and treated in 5% bovine serum albumin for 1 h. After o/n incubation of primary antibodies, secondary antibodies conjugated with Alexa Fluor 595, Alexa Fluor 488, or Texas red were then added to the samples and incubated for 1 h at 20 °C. The slides were incubated with DAPI for 5 min and mounted in glycerol following repeated PBS washes. Images were taken by EVOS system (Advanced Microscopy Group, Bothell, WA, USA).

Wound healing assay

Migration was assessed using a wound-healing assay. Three days were given for the cells to grow in six-well plates from the time of seeding till full confluence. At 0 h, the media were removed, and we made a scratch on the cell plate using a 200 μl pipette tip. Cell debris was washed off twice with PBS, fresh medium was added, and plates were again incubated at 37 °C for 48 h. After 0, 48 and 72 h or scratch wounding, microscopy pictures were captured under an inverted phase-contrast microscope. All experiments were repeated thrice. Using ImageJ software, the results were quantitated from the images.

Transwell migration assay

Serum-starved A549 cells were cultured in DMEM with 1% FBS overnight. Cells (6×10^4/well) were seeded on Transwell inserts of an 8 μm pore size with 2% FBS (negative control) with or without 10 ng/mL TGF-β1 (stimulant, positive control) so that the cells can be transferred to the lower chamber of a 24-well plate. After the wells were incubated for 24 h in a 37 °C CO2 incubator, the Transwell inserts were taken out. Wet cotton swabs were used to remove the remaining cells that had not migrated from the top of the insert. The samples were stained with crystal violet after being fixed with 4% paraformaldehyde for 10 min.

Determination of ROS generation

The DCFDA test, which uses 2′,7′-dichlorofluorescein diacetate to measure intracellular ROS levels, was used. The cells were subjected to their various treatments for the times specified, and then incubated with DCFDA (10 μM) in media for 30 min at 37 °C. A microplate spectrophotometer plate reader (GENios, TECAN Group, Maennedorf, Switzerland) operating at Ex/Em 502/535 nm was used to read the fluorescence that was released.

Sirius Red staining

A549 cells were seeded 5000 cells per well into 96-well culture and then in the middle of the process, two and four days after seeding, the cells were serum-starved in DMEM containing 2% FBS and treated with 20 μg/mL bleomycin or TMF (2 μM) and CAT (2 μM) containing 1% FBS. After five days of treatment, the cells were fixed with 4% buffered paraformaldehyde in PBS. Then, 50 μL of staining solution was added to each well for 1 h.

Experimental mice

Seven-week-old male C57BL/6 J mice weighing 20–25 g were purchased from Daehan Biolink (Chung-cheong bukdo, Republic of Korea). The animals were raised under a 12 h day-12 h night cycle in a well-ventilated room at 22 ± 2 °C with the guidelines of the Animal Care and Use Committee (WJIACUC20191206-4-35) of Woojung Bio, Republic of Korea. After a seven-day adaptive feeding, the randomized mice were divided into five groups (n = 8 mice per group) as follows: 1. Normal saline (NS), 2. BLM, 3. BLM + TMF (10 mg/kg), 4. BLM + CAT (0.5 mg/kg) and 5. BLM + TMF (10 mg/kg) / CAT (0.5 mg/kg). On day 0, a single intratracheal instillation of 50 μL saline

containing BLM (3 mg/kg) was administered to induce pulmonary fibrosis in the mice. Mice in the control (NS) group received an equal volume of saline. One day after BLM induction, mice in the TMF, CAT, and TMF/CAT groups were intragastrically administered TMF or CAT for 28 days. On day 29, all animals were euthanized and lung tissues and blood were collected for subsequent studies.

Histopathological analysis
On lung samples, hematoxylin and eosin (H&E) and Masson's trichrome staining were done. Using an Olympus BX51 microscope, three separate sites were used to collect H&E and trichrome stained lung pictures. The Ashcroft score was measured using these photographs. Using a preset scale of severity, the interstitial fibrosis severity was evaluated for each field separately and given a score between 0 and 8. The fibrosis score for each site was calculated after the entire section had been examined.

ELISA
LAP1, latent TGF-1, or TGF-1 in 100 μl PBS were coated for 16 h at 4 °C on 96-well plates (NEST, Wuxi, Jiangsu, China). The wells were coated and then blocked with an incubation solution (PBS with 0.05% Tween 20 and 0.1% bovine serum albumin) for 1 h. Goat-anti-mouse IgG Alkaline Phosphatase Conjugate (Invitrogen, Carlsbad, CA, USA) was then added and incubated for 1 h. Next, para-nitrophenyl phosphate (Sigma-Aldrich, St. Louis, MO, USA) was used for development, and then an ELISA reader was used to detect absorbance (405 nm) (GENios, TECAN Group). Five washes with PBS with 0.1% Tween 20 were performed between the assay steps.

BALF analysis
Mice were anesthetized and 1 ml syringe was used for the lavage, being filled and emptied five times in a row with pre-warmed (37 °C) PBS for cycle 1. For cycles 2–5, PBS with 0.325% bovine serum albumin was used. 1 cc of lavage medium was used to fill and empty each cycle, and the process was then repeated. Cycle 1's supernatant was collected by centrifuging $300 \times g$ for 5 min at 4 °C, then freezing it in aliquots at -70 °C. In order to identify and count cell subpopulations, samples of bronchoalveolar lavage fluid leukocytes, which were present in the cell pellet from cycle 1 along with the entire cell suspension from cycles 2–5, were stored at 4 °C.

RNA isolation and quantitative RT-PCR (qPCR)
Total RNA was extracted from the mice lung tissues using TRIzol reagent (Invitrogen, Carlsbad, CA, USA),

according to the manufacturer's protocol. Quantitative RT-PCR was conducted for the synthesis of cDNA using a reverse transcriptase kit (Promega, Seoul, Republic of Korea).

Real-time polymerase chain reaction
Total RNA isolation and cDNA synthesis were performed as described previously. Using SYBR Green Master Mix (KAPA BIOSYSTEMS, Cape Town, South Africa), Real-time PCR was carried out as directed by the manufacturer.

Sequence of the human gene specific primers used were as below:

IL-1β sense primer, 5'- CCACCTCCAGGGACAGGATA-3';

IL-1β antisense primer, 5'- AACACGCAGGACAGGTACAG-3';

IL-13 sense primer, 5'- CCTCATGGCGCTTTTGTTGA -3'.

IL-13 antisense primer, 5'- TGCCAGCTGTCAGGTTGATG -3';

TNF-α sense primer, 5'- ATCCTGGGGGACCCAATGTA -3';

TNF-α antisense primer, 5'- AAAAGAAGGCACAGAGGCCA -3';

β-actin sense primer: 5'- TGGAACGGTGAAGGTGACAG -3';

β-actin antisense primer 5'- AACAACGCATCTCATATTTGGAA -3'.

Real-time qRT-PCR was performed using the StepOne Real-Time PCR System (Applied Biosystems, Waltham, MA, USA).

Statistical analysis
All experiments were repeated three times. Statistical analyses were performed using Excel (Microsoft, Redmond, WA, USA). Data are expressed as means ± standard deviation (SD). Statistical significance was set at $p < 0.05$.

Results
TMF and CAT do not affect the viability of several types of cell lines
MTT assays were performed to determine the influence of TMF and CAT on the viability of several cell lines. For the A549 cell line which was the main cell in our subsequent experiments, TMF and CAT were treated at concentrations of 5 to 40 μM and 0.5 to 5 μM, respectively, and for the co-treatment, concentrations of 5/0.25, 5/0.5, 10/0.25, and 10/0.5 μM of TMF/CAT were used. The same experimental groups and conditions were used for 24 and 48 h, respectively.

TMF and CAT did not significantly affect cell viability in any of the treatment groups, except for 5 μM CAT alone at 48 h (Fig. 1D).

The intoxicity of TMF and CAT was also examined in other cell lines, such as myoblast (C2C12) and fibroblasts (HDF, MRC-5), by the MTT assay. The concentrations of TMF and CAT were 10 and 0.5 μM, respectively, for single treatment, and 10/0.5 μM of TMF/CAT for the co-treatment. Here, TMF and CAT did not affect viability at either 24 h or 48 h (Fig. 1E).

TMF and CAT show inhibitory effects on TGF-β1-induced in vitro fibrosis

Using the MTT assay, we were able to select appropriate concentrations of TMF and CAT that were not toxic to cells. We treated A549 cells with these concentrations to determine whether they have any antifibrotic effect on in vitro fibrosis induced by TGF-β1.

The efficacy of TMF and CAT was confirmed by observing the morphology of A549 cells. The cobblestone shape in the control group changed to an elongated, spindle-like profibrotic phenotype by TGF-β1, and this change was attenuated by TMF/CAT single or co-treatment (Fig. 2A).

Western blotting was performed to confirm whether changes in protein expression were related to changes in cell morphology. After treating cells with TGF- β1, changes in the factors of the canonical and non-canonical signaling pathways were observed. ECM production and EMT progression, which are the result of these pathways, were also confirmed. The cells were treated with the chemicals for at least 24 h to observe several consequential results, including the production of ECM, and the treatment was conducted for up to 48 h, which is less than the time it takes for the cells to enter senescence. TMF and CAT showed antifibrotic effects at both 24 and 48 h of treatment, as can be seen in the decrease of COL4A6 and α-SMA (Fig. 2B). Whether a single administration or co-administration is better, varied slightly depending on the observing factor, but the antifibrotic effect was observed well in the co-administration.

After 24 h, changes in the expression of various fibrosis-specific and mesenchymal cell-specific markers were observed again. Here, it could be seen that TMF and CAT were effective in fibrosis mitigation and EMT inhibition (Fig. 2C). We also examined the changes in the expression of integrin beta 3 and Cyr61. The integrin family of cell adhesion receptors has gained prominence as a key regulator of chronic inflammation and fibrosis [18]. Among the family members, we observed a change in the expression of integrin beta 3. For Cyr61, which acts as an ECM-associated signaling molecule, we could confirm that Cyr61 was expressed more when TGF-β1 was treated compared to that in the control group. We examined whether TMF and CAT had similar antifibrotic effects on the expression of Cyr61. In addition, mitogen-activated protein kinase (MAPK) signaling pathway-specific markers and NOX2 were observed, and TMF and CAT showed similar inhibitory effects.

Several factors were identified after 48 h of treatment (Fig. 2C). TMF and CAT showed their effects in line with previous results, and the expression of NOX2 was also reduced, thereby reducing the generation of ROS. Their antifibrotic effects can be compared to those of nintedanib, one of only two FDA-approved drugs available for the treatment of IPF.

The inhibitory effects of TMF and CAT on in vitro fibrosis was confirmed by immunofluorescence (Fig. 2D). TMF and CAT reduced the expression of α-SMA which was increased by TGF-β1. Simultaneously, they restored the expression of E-cadherin, which was reduced by TGF-β1, indicating that they inhibited the EMT of A549 cells.

This EMT-inhibitory effect of TMF and CAT was proven again through wound healing (Fig. 2E) and transwell migration assays (Fig. 2F), which can measure the

(See figure on next page.)
Fig. 2 TMF and CAT attenuate TGF-β1-induced fibrosis in A549 cells with decreasing EMT. **A** The morphology of A549 cells was observed by 100 × microscopy, after 48 h of treating TGF-β1 (10 ng/ml) with or without TMF (2 μM) and CAT (2 μM). **B** Western blot results of treating A549 cells with TGF-β1 for 24 or 48 h, together with TMF or CAT. The graph shows the relatively quantified value of western blot results if that of non-TGF-β1-treated group against GAPDH was 1. **C** Specific time (24 h) was selected and A549 cells were treated with TGF-β1, TMF and CAT. Changes in expression of various factors were observed. Another specific time (48 h) was selected to treat A549 cells with TGF-β1, TMF and CAT. The generation of ECM by the canonical signaling pathway, the degree of progress of non-canonical signaling pathway, and the expression of NOX2 were observed. **D** After treating TGF-β1 with or without TMF and CAT for 48 h, the cellular levels of α-SMA (red) and E-cadherin (E-cad, green) were observed. For each observation, a merged image with DAPI is also shown. **E** The EMT inhibitory effects of TMF and CAT were confirmed through the wound healing assay. Compared to the time prior to treatment, microscopic images of 72 h treatments are presented in which the scratched wounds were closed according to the cell migration. For each 48 and 72 h treatment, assuming that when the wound is completely closed means 100%, the relative degree of closure of each treatment group is presented as a graph. **F** It was confirmed again that TMF and CAT inhibited EMT of A549 cells, through the transwell migration assay. We counted the cells that migrated across the permeable membrane from the upper layer of cell culture during the treatment
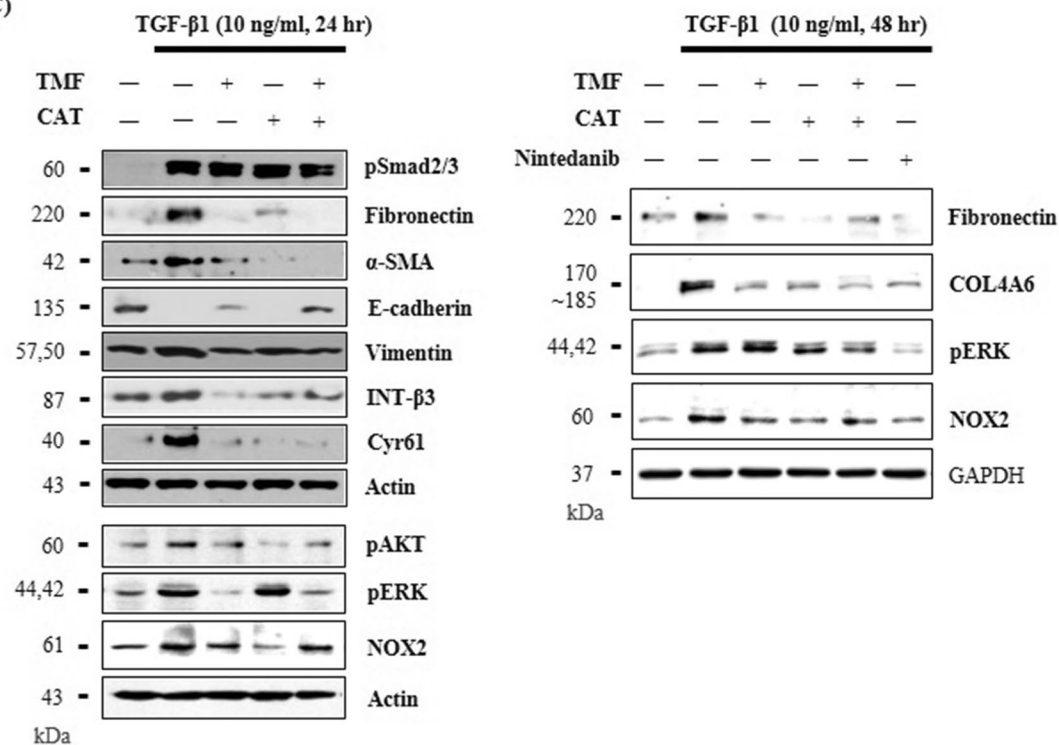
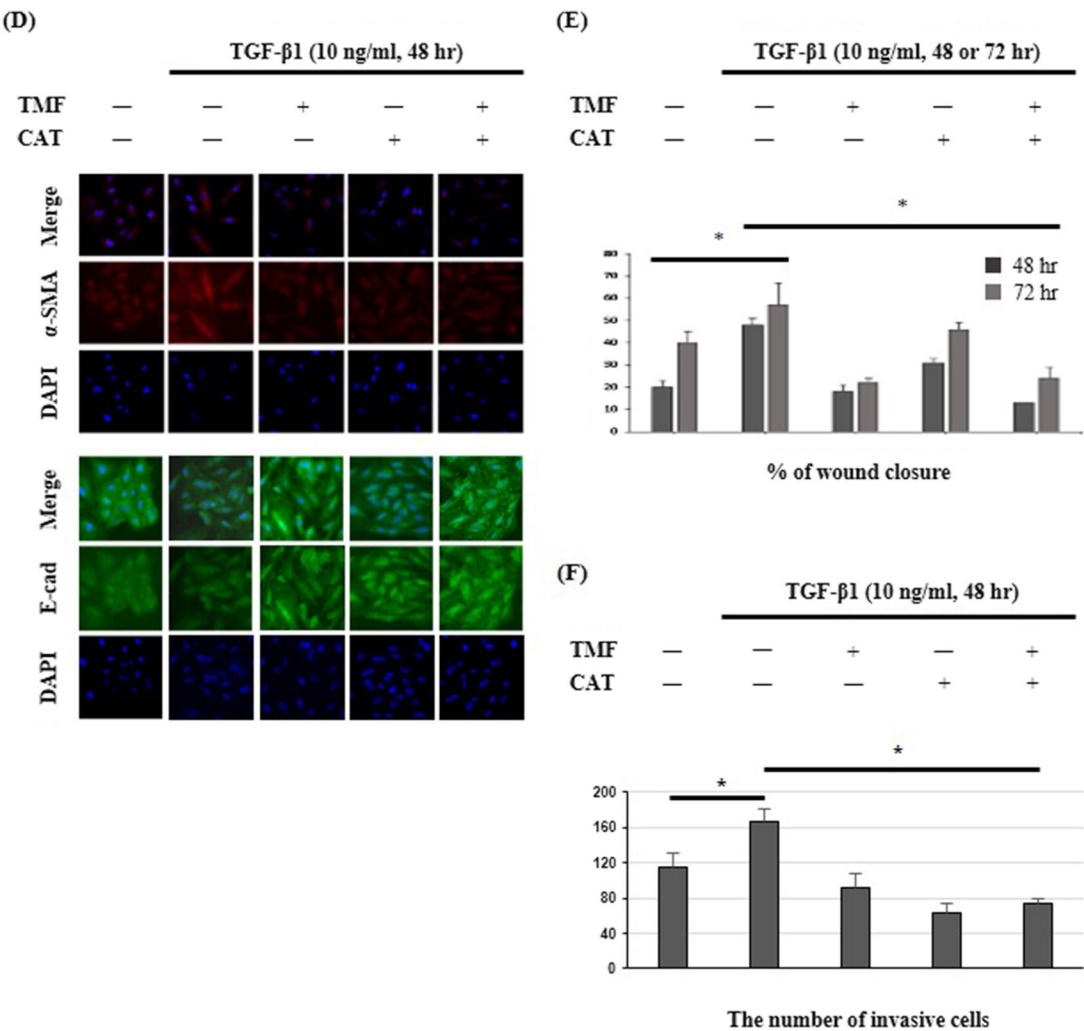Choi *et al. Applied Biological Chemistry*   (2023) 66:9

Page 7 of 15
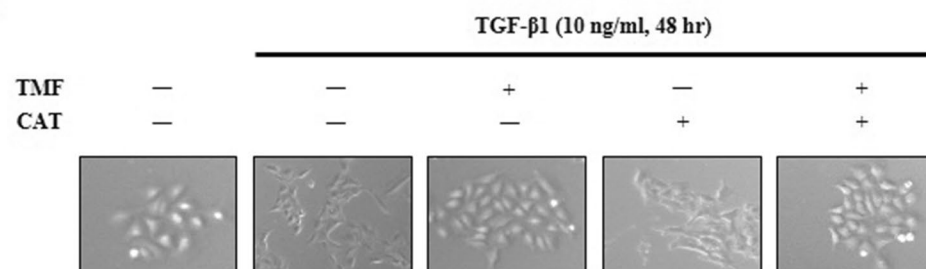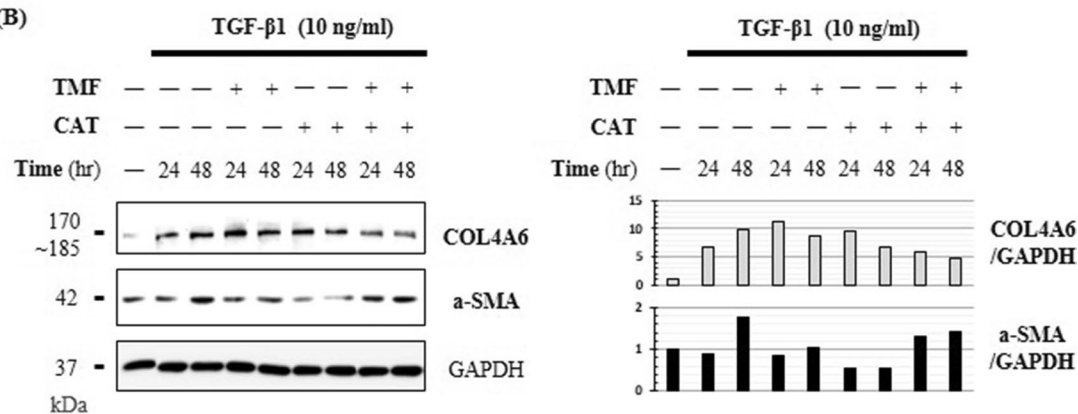
Fig. 2 continued

mobility of A549 cells treated with TGF-β1, TMF, or CAT. When TGF-β1 was treated, it could be seen that the migration of the cells increased in response to that, along with the progress of EMT, and this movement was inhibited by TMF and CAT.

BLM can induce fibrosis in A549 cells with the increase of ROS and NOX2 expression

It is well known that pulmonary fibrosis induced by BLM occurs in the in vivo model, and the induction method is also well established. However, the effects of BLM in in vitro experiments are not well known. Here, we attempted to treat cells with BLM to induce fibrosis in A549 cells.

After 48 h, we treated cells with BLM at various concentrations of 5–80 μg/ml and observed that α-SMA, the fibrotic marker, was increased accordingly (Fig. 3A).

It was confirmed that the expression level of α-SMA was increased by BLM, and at the same time, the level of E-cadherin was decreased. Another notable point is that BLM induced fibrosis and increased the expression of NOX2. This was expected to lead to an increase in ROS, as confirmed by the DCF-DA assay (Fig. 3B).

When BLM was treated with various concentrations of 10–100 μg/ml for 48 h, ROS were generated in a concentration-dependent manner.

The effect of BLM on A549 cells was confirmed using immunofluorescence (Fig. 3C). BLM increased the expression of α-SMA (red) and NOX2 (green) while decreasing the expression of E-cadherin (green).

TMF and CAT reduce NOX2 expression and in vitro fibrosis induced by BLM

As previously confirmed, in vitro fibrosis can be induced by BLM, and ROS production and NOX2 expression
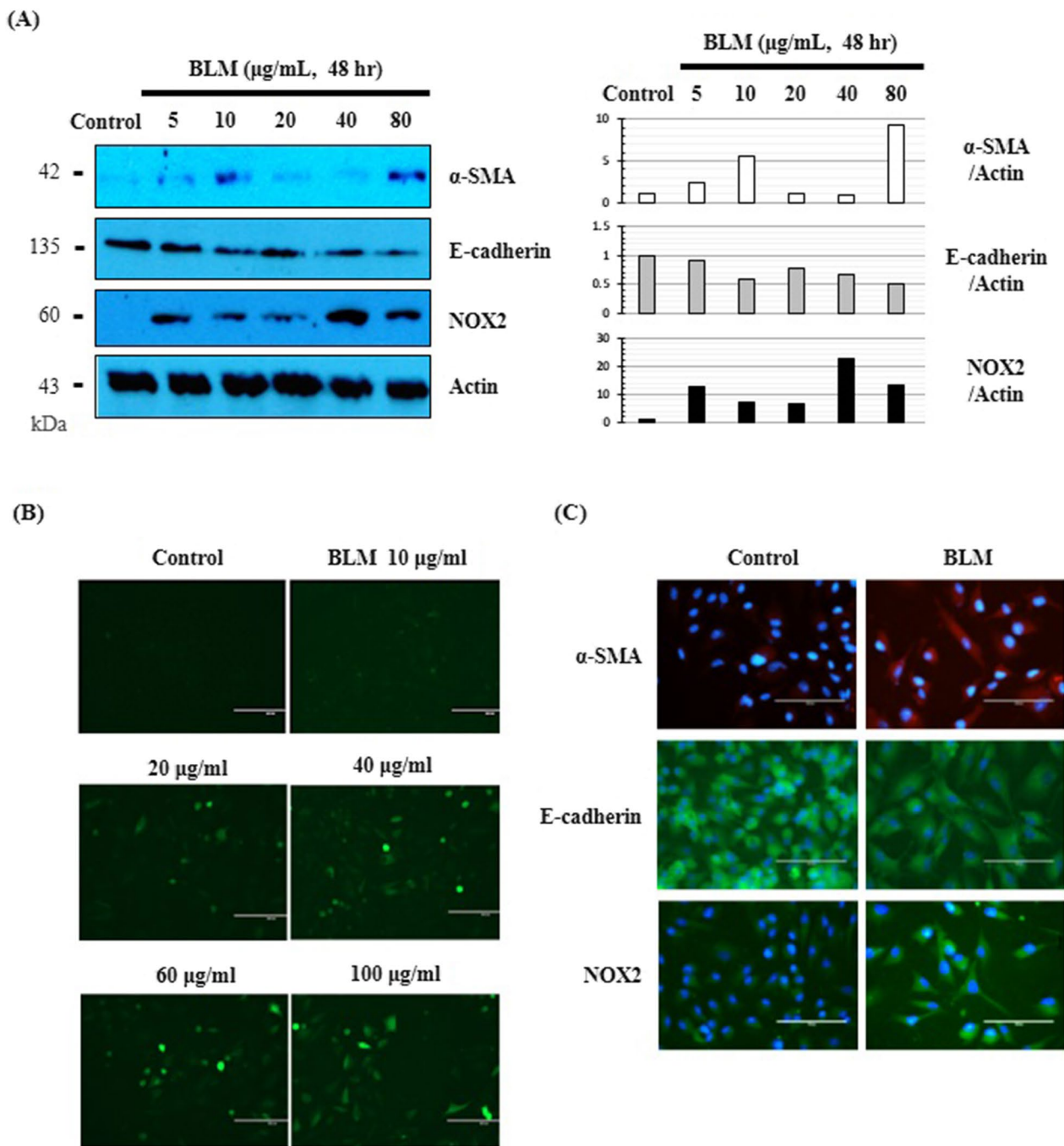
Choi *et al. Applied Biological Chemistry*   (2023) 66:9

Page 9 of 15

Fig. 3 BLM increases α-SMA and NOX2 expression while decreasing E-cadherin in A549. **A** A549 cells were treated with BLM with concentrations of 5, 10, 20, 40, 80 μg/ml for 48 h. The graph shows the relatively quantified value of western blot results if that of the control group against actin was 1. **B** We treated BLM of 10, 20, 40, 60, 80, 100 μg/ml for 48 h and replaced the media with DCF-DA (10 μM) dissolved PBS. The images are observed under the 100 × fluorescence microscope. **C** After treating BLM (20 μg/ml) for 48 h, the cellular levels of α-SMA (red), E-cadherin (green) and NOX2 (green) were observed by immunofluorescence and the images are shown compared to the control group

are increased during this process. We then investigated whether TMF and CAT have similar effects against BLM-induced in vitro fibrosis and TGF-β1-induced fibrosis.

After 24 h of treatment with BLM (Fig. 4A), the expression of NOX2 increased, which would have led to an increase in ROS generation (Fig. 4B). This increase coincided with the early stimulation of non-canonical

Choi *et al. Applied Biological Chemistry*   (2023) 66:9

Page 10 of 15

signaling pathways downstream of TGF-β1. TMF and CAT effectively decreased NOX2 expression and arrested stimulation of the pathways.

After 48 h of treatment with BLM (Fig. 4B), NOX2 expression increased, as in the 24 h treatment. We observed several consequential factors of the canonical and non-canonical signaling pathways, such as fibrosis-specific markers and E-cadherin. The efficacy of TMF and CAT in reducing NOX2 expression was accompanied by decreases in fibronectin, α-SMA, and EMT.

To analyze the level of collagen, which is used as a marker of fibrosis, a Sirius Red staining assay was conducted (Fig. 4C). A549 cells were treated for 5 d with BLM or TMF/CAT. The cells were stained with Sirius Red reagent and observed under a microscope. Although BLM increased collagen production, TMF and CAT attenuated this increase. The graph shows the quantified red fluorescence intensity in the microscopic images.

The degree of EMT and the resulting cell mobility were observed by the transwell migration assay when treated with BLM or TMF/CAT (Fig. 4D). After 72 h, cell migration increased and was reduced by TMF and CAT. This was similar to the results of TGF-β1 treatment in Fig. 3F. The graph shows the number of invasive cells on each plate.

TMF and CAT have antifibrotic and anti-inflammatory effects against BLM-induced pulmonary fibrosis in a mouse model

Previous experiments have shown that TMF and CAT have inhibitory effects on TGF-β1- and BLM-induced in vitro fibrosis. We then investigated whether these were still effective in the in vivo fibrosis induced by BLM. Eight mice per group were intraperitoneally injected with BLM or TMF/CAT for three weeks. After they were euthanized, the lung tissues and serum were collected, and the following experiments were conducted.

The degree of collagen deposition was observed by H&E and Masson's trichrome staining using lung tissue slides (Fig. 5A). In each staining, the level of collagen was significantly increased by BLM treatment, confirming BLM-induced pulmonary fibrosis. When TMF or CAT were injected together with the same BLM concentration, the increase in collagen deposition was remarkably alleviated. Graph in Fig. 5A shows the Ashcroft score, which was assigned based on both straining pictures. BLM significantly increased the Ashcroft score compared to that of the control, indicating that BLM caused fibrosis in mouse lungs. The increase in the score was reduced by TMF and CAT.

The antifibrotic effects of TMF and CAT were also confirmed by western blotting after homogenizing lung tissue (Fig. 5B). Similar to BLM-induced in vitro fibrosis, BLM increased the expression of fibrotic markers and promoted EMT progression. TMF and CAT decreased the expression of fibronectin and α-SMA and restored the expression of E-cadherin. The TMF/CAT co-treatment had the most significant effects.

In addition, the amount of TGF-β1 in mice serum which can be influenced by BLM injection, was investigated using ELISA and shown in Fig. 5C. As shown here, TMF and CAT could reduce the generation of TGF-β1.

Fibrosis is inevitably accompanied by inflammation. Thus, the effect of inhibition of fibrosis can also be confirmed by the degree of inhibition of inflammation. To evaluate the efficacy of TMF and CAT against inflammation, the number of inflammatory cells and the levels of inflammatory cytokines were investigated.

Changes in the amount of bronchoalveolar lavage (BAL) fluid (BALF) reflect pathological changes in the lung parenchyma. BALF is largely occupied by inflammatory cells present in the alveolar space, especially macrophages, lymphocytes (LYM), and neutrophils (NEU). In BALF analysis, BLM significantly increased the total cell count (Fig. 5D). Moreover, recognizing the changes in the predominant inflammatory cells in BALF frequently helps us associate it with some interstitial lung diseases, such as IPF. In this BALF analysis, we observed that while BLM increased the total cell number in BALF, it also increased the proportion of lymphocytes; this increase was reduced by TMF and CAT. This indicated that TMF and CAT alleviated inflammation.

The number of inflammatory cells and mRNA levels of proinflammatory cytokines were determined by quantitative RT-PCR (qRT-PCR). Figure 5E shows the normalized fold mRNA levels of IL-1β, IL-13, and TNF-α in BLM-challenged lungs compared to those in the control group. BLM significantly increased the expression

(See figure on next page.)

Fig. 4 TMF and CAT result in a decrease of BLM-induced fibrosis and NOX2 expression. **A**, **B** BLM (20 μg/ml) significantly increased the NOX2 expression under both 24 and 48 h treatments. In the 24 h treatment, the change of non-canonical signaling pathways' factors were observed. TMF and CAT alleviated the stimulated PI3K/AKT, ERK and p38 pathways. In the 48 h treatment, the antifibrotic and anti-EMT effect of TMF and CAT were confirmed. The graph shows the relatively quantified value of western blot results if that of the control group against actin was 1. **C** In the Sirius Red staining assay, BLM for 5 d increased collagen production in A549 cells, as can be seen by the increase of red intensity. TMF and CAT reduced that increase. The graph shows the relative red intensity in the 100 × microscopic images. **D** In the transwell migration assay, we could observe TMF and CAT inhibiting EMT of A549 cells induced by BLM (20 μg/ml, 72 h). We counted the number of invasive cells across the permeable membrane from the upper layer of cell culture during the treatment
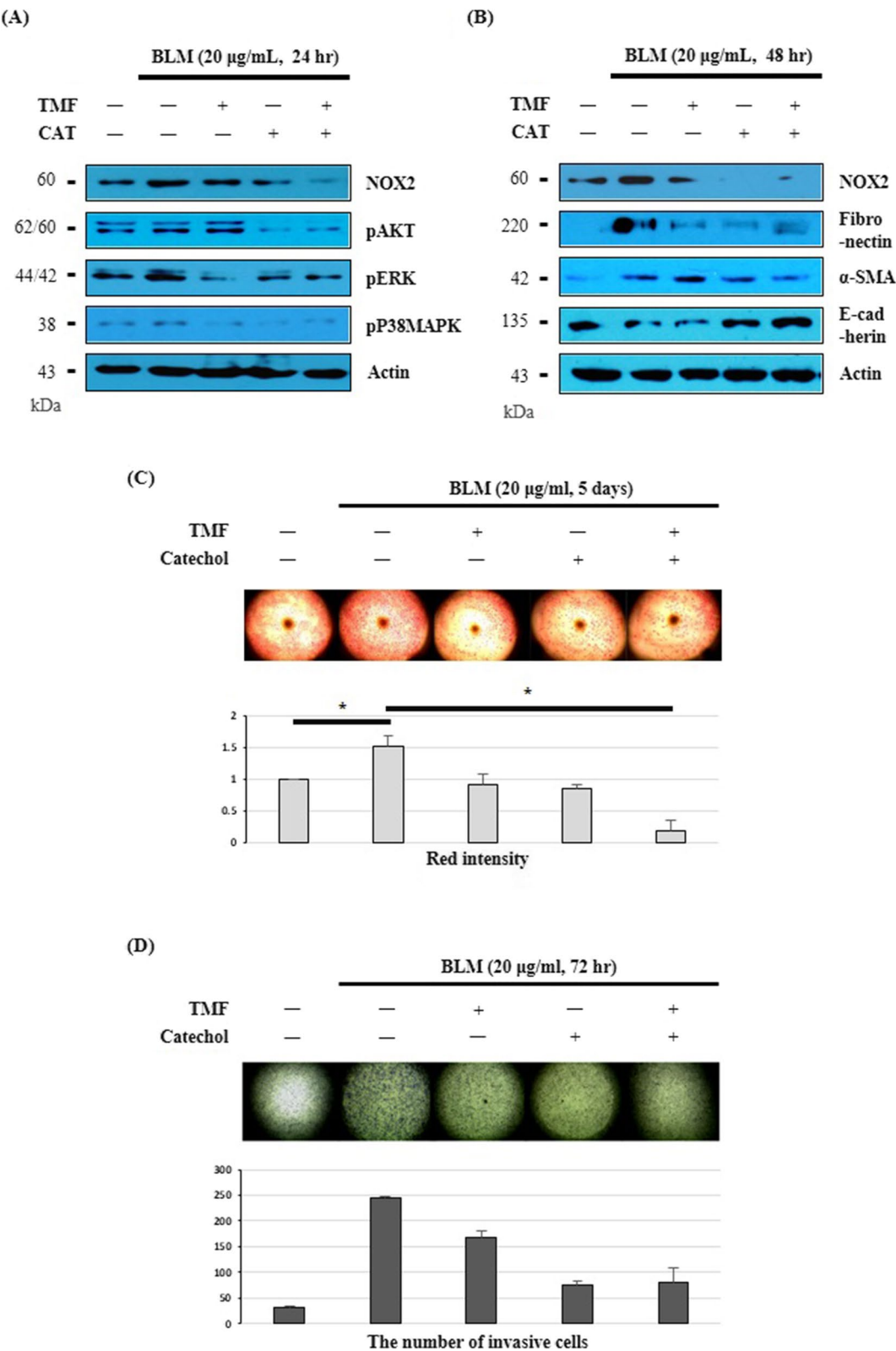
Choi *et al. Applied Biological Chemistry*   (2023) 66:9

Page 11 of 15

Fig. 4 (See legend on previous page.)

Choi *et al. Applied Biological Chemistry*   (2023) 66:9

Page 12 of 15

of these proinflammatory cytokines at the mRNA level, whereas TMF and CAT reduced their expression.

Discussion

We examined the possibility that TMF and CAT could act as antifibrotic agents. Their safety was confirmed in various cell lines, and with safe concentrations. Based on this, in vitro and in vivo experiments were conducted. TMF and CAT showed antifibrotic effects on in vitro fibrosis induced by TGF-β1 or BLM and in vivo fibrosis induced by BLM.

Flavonoids, including TMF, have attracted attention because of their ability to reduce free radical formation and scavenge free radicals. In our previous study, we screened more than one hundred flavonoids based on their capacity for wound healing, and TMF was one of the compounds that showed the best ability to regulate NOX expression [19]. In another study, TMF showed excellent efficacy in mitigating the expression of TGF-β1 by fibroblasts, which were derived from hypertrophic scars of the impaired burn wound model in mice [17]. Based on these results, we hypothesized that TMF could inhibit fibrosis.

The beneficial effect of CAT in enhancing the radical scavenging activity of flavonoids and other phenolics has been verified by many studies performed in diverse systems [14]. CAT acts as a reductant, causing free radicals to be reduced to a more stable form. TMF also contains CAT in its structure, and we tested its efficacy by adding chemically purified CAT to the antifibrotic drug candidate group.

To confirm the safety of utilizing these two chemicals as drugs, an in vitro MTT assay using A549 cells was performed. The two chemicals were treated individually or in combination at various concentrations for 24 or 48 h. Their safety was also confirmed using cell lines, such as fibroblasts and myocytes. Some studies have reported the cytotoxicity of CAT [20, 21] and DNA damage caused by CAT-induced DNA adduct formation or ROS production [22]. However, this does not apply at the low concentrations (less than 5 μM) that we tested, for its potential as an antifibrotic drug. The DNA damage mentioned also occurs only with the activation of CAT by heavy metals or with cellular metabolism and conjugation reactions that occur when high concentrations of CAT (more than 10 μM) are used [22].

The efficacy of TMF and CAT in inhibiting fibrosis was demonstrated in TGF-β1- and BLM-induced in vitro fibrosis experiments using A549 cells. These were performed under concentration and time conditions, which were shown to be non-toxic in the MTT assay. TMF and CAT decreased the expression of fibrosis factors and EMT (Figs. 3 and 5).

EMT is accelerated by ROS. One study showed that an intermediate amount of ROS can trigger the activation of nuclear factor kappa B (NF-κB), which is considered a pivotal regulator of the EMT process [23]. Another study further confirmed the relationship between ROS, zinc finger protein SNAI1 expression, and E-cadherin downregulation in MCF-7 cells [24]. Based on these results, we assumed that the decrease in ROS by TMF and CAT could make an EMT-inhibitory effect.

TMF was especially effective in alleviating TGF-β1- and BLM-induced increase in non-canonical signaling pathway factors (Fig. 3C, 5A). As TMF is a flavonoid, one of its functions is to interact with a range of protein kinases that supersede the key steps of cell growth and differentiation [25]. TMF is presumed to affect the activities of protein kinases, such as MAPK, and other non-canonical signaling pathway factors.

In addition to this inhibition across both canonical and non-canonical signaling pathways, it is noteworthy that TMF and CAT reduced the expression of NOX itself (Figs. 3D, 5A, B). Our previous study confirmed that downstream signaling pathways of TGF-β increase NOX expression, in which TGF-β augments its transcriptional activity toward NOX2 and NOX4 via integrin [26]. From the perspective of redox-fibrosis, a decrease in ROS due to inhibition of NOX expression would contribute significantly to alleviating the consequential fibrosis.

BLM has been used in animal studies to model pulmonary fibrosis. Because ROS play a significant role in the process of BLM causing fibrosis, we tried to apply it to in vitro experiments and obtained the results in our previous work. We confirmed that the injury and inflammation imposed on A549 cells by BLM-induced ROS exposure activated latent TGF-β. Mature TGF-β initiates

(See figure on next page.)

Fig. 5 TMF and CAT show effects against fibrosis and inflammation in BLM-challenged mice lungs. **A** Representative images of pulmonary tissues stained with hematoxylin and eosin (H&E) or Masson's trichrome staining. Each specimen was photographed under 50 × microscopy. The graph shows the Ashcroft score which was assigned based on those two types of staining images. **B** Western blot results of homogenized lung tissue show antifibrotic effects of TMF and CAT. The bands here include two samples for each treatment group and the graph reflects two of each, showing their average. **C** The concentration of TGF-β1 (pg/ml) in mice serum of each group was investigated by sandwich ELISA and the graph shows the average calculated value. **D** Analysis of total cell numbers and types (NEU, LYM and macrophage) in BALF. BALF analysis was performed in mice after three weeks of treatment of each. **E** qRT-PCR results using lung tissue show the normalized fold mRNA expression of IL-1β, IL-13 and TNF-α relative to actin
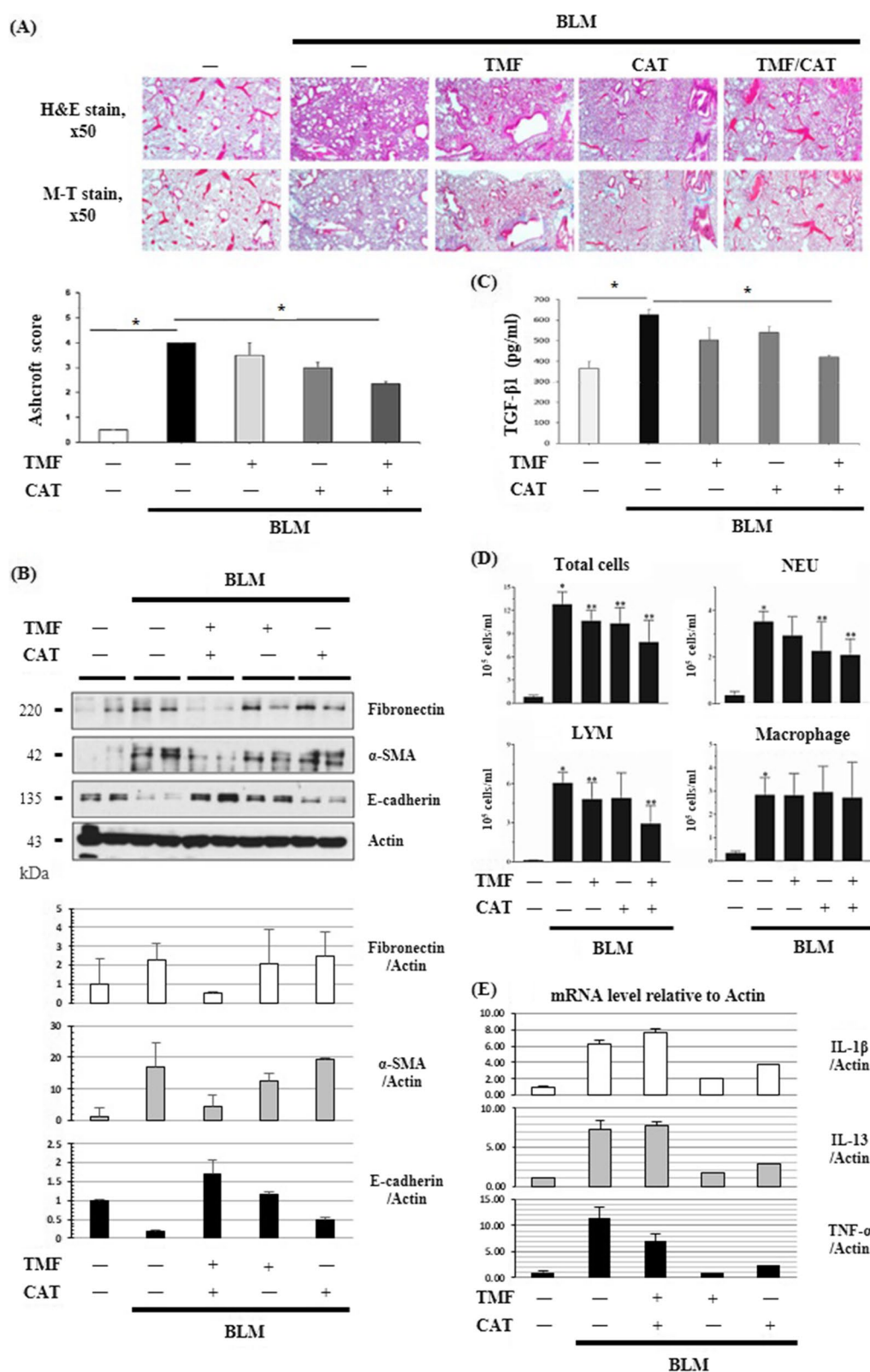
Fig. 5 (See legend on previous page.)

Choi *et al. Applied Biological Chemistry*   (2023) 66:9

Page 14 of 15

integrin activation and causes an imbalance in the redox state of the cell, aggravating fibrotic conditions [26]. It was also seen in Fig. 5C that being challenged by BLM, TGF-β1 content increased in vivo. Meanwhile, TMF and CAT had significant antifibrotic and anti-inflammatory effects in BLM-induced in vivo models.

N-acetylcysteine (NAC) has been suggested as a beneficial treatment for IPF. The primary role of NAC is associated with its antioxidant and anti-inflammatory activities, which favor the maintenance of cellular redox imbalance [27]. The effectiveness of NAC therapy for IPF, however, is still debatable, according to earlier clinical investigations. NAC therapy may aid in delaying the decline in lung function, according to some research, while other studies have found no benefit for IPF patients from this medication [28].

TMF and CAT were also noted for their antioxidant properties like NAC; however, we need to focus on the difference between them: TMF's ability to control the activity of several protein kinases. Among these kinases, several growth factor receptors, such as epidermal growth factor receptors (EGFRs) or fibroblast growth factor receptors (FGFRs), have ATP-binding sites. The point is that these sites are partly occupied by TMF, if not completely, or not occupied as much as nintedanib. Thus, TMF inhibits sulfenylation near the ATP binding site, thus decreasing receptor tyrosine kinase activity [29]. In other words, it is assumed that TMF and CAT act as antioxidants and at the same time, TMF has another mechanism to inhibit the downstream processes of several GFRs. However, a detailed and accurate exploration of their mechanisms of action is needed. If the difference with NAC in how TMF and CAT work is explored precisely, it will bring about a meaningful discussion of future fibrosis medicine candidates.

Conclusion
In conclusion, this study investigated the therapeutic effects of TMF and CAT against pulmonary fibrosis. These effects were observed in both in vitro (TGF-β1 and BLM-induced) and in vivo (BLM-induced) experiments. These results suggest that TMF and CAT, alone or in combination, significantly decreased the expression of fibrotic proteins and inflammatory cytokines. This overall decrease eventually results in attenuation of fibrosis.

Declarations

Competing interests
The authors declare that they have no competing interests.

References
1. Henderson NC, Rieder F, Wynn TA (2020) Fibrosis: from mechanisms to medicines. Nature 587(7835):555–566
2. Hinz B (2007) Formation and function of the myofibroblast during tissue repair. J Investig Dermatol 127(3):526–537
3. Wynn TA, Ramalingam TR (2012) Mechanisms of fibrosis: therapeutic translation for fibrotic disease. Nat Med 18(7):1028–1040
4. Wight TN, Potter-Perigo S (2011) The extracellular matrix: an active or passive player in fibrosis? Am J Physiol Gastrointest Liver Physiol 301(6):G950–G955
5. Sauleda J, Núñez B, Sala E, Soriano J (2018) Idiopathic pulmonary fibrosis: epidemiology, natural history, phenotypes. Med Sci 6(4):110
6. Ma Z, Zhao C, Chen Q, Yu C, Zhang H, Zhang Z, Huang W, Shen Z (2018) Antifibrotic effects of a novel pirfenidone derivative in vitro and in vivo. Pulm Pharmacol Ther 53:100–106
7. Birben E, Sahiner UM, Sackesen C, Erzurum S, Kalayci O (2012) Oxidative stress and antioxidant defense. World Allergy Organ J 5(1):9–19
8. Richter K, Konzack A, Pihlajaniemi T, Heljasvaara R, Kietzmann T (2015) Redox-fibrosis: impact of TGFβ1 on ROS generators, mediators and functional consequences. Redox Biol 6:344–352
9. Richter K, Kietzmann T (2016) Reactive oxygen species and fibrosis: further evidence of a significant liaison. Cell Tissue Res 365(3):591–605
10. Yang D-P, Ji H-F, Tang G-Y, Ren W, Zhang H-Y (2007) How many drugs are catecholics. Molecules 12(4):878–884
11. Ullah A, Munir S, Badshah SL, Khan N, Ghani L, Poulson BG, Emwas AH, Jaremko M (2020) Important flavonoids and their role as a therapeutic agent. Molecules 25(22):5243
12. Yuan J, Li W, Tian Y, Wang X (2012) Anti-proliferative effect of Flos Albiziae flavonoids on the human gastric cancer SGC-7901 cell line. Exp Ther Med 5(1):51–56
13. Pietta P-G (2000) Flavonoids as antioxidants. J Nat Prod 63(7):1035–1042
14. Zhang H-Y (2005) Structure-activity relationships and rational design strategies for radical- scavenging antioxidants. Curr Comput Aided-Drug Des 1(3):257–273
15. Novaes P, Torres PB, Cornu TA, de Lopes JC, Ferreira MJP, dos Santos DYAC (2019) Comparing antioxidant activities of flavonols from Annona coriacea by four approaches. S Afr J Bot 123:253–258
16. Sarkar A, Middya TR, Jana AD (2011) A QSAR study of radical scavenging antioxidant activity of a series of flavonoids using DFT based quantum chemical descriptors—the importance of group frontier electron density. J Mol Model 18(6):2621–2631
17. Seo GY, Lim Y, Koh D, Huh JS, Hyun C, Kim YM, Cho M (2017) TMF and glycitin act synergistically on keratinocytes and fibroblasts to promote wound healing and anti-scarring activity. Exp Mol Med 49(3):e302–e302

18. Henderson NC, Sheppard D (2013) Integrin-mediated regulation of TGFβ in fibrosis. Biochimica et Biophysica Acta (BBA) Mol Basis Dis 1832(7):891–896

19. Bui NT, Ho MT, Kim YM, Lim Y, Cho M (2014) Flavonoids promoting HaCaT migration: II. Molecular mechanism of 4′,6,7-trimethoxyisoflavone via NOX2 activation. Phytomedicine 21(4):570–577

20. de Oliveira DM, Pitanga BP, Grangeiro MS, Lima RM, Costa MF, Costa SL, Clarêncio J, El-Bachá RS (2010) Catechol cytotoxicity in vitro: Induction of glioblastoma cell death by apoptosis. Hum Exp Toxicol 29(3):199–212

21. Vazhappilly CG, Hodeify R, Siddiqui SS, Laham AJ, Menon V, El-Awady R, Matar R, Merheb M, Marton J, Al Zouabi HAK, Radhakrishnan R (2020) Natural compound catechol induces DNA damage, apoptosis, and G1 cell cycle arrest in breast cancer cells. Phytother Res 35(4):2185–2199

22. Schweigert N, Zehnder AJB, Eggen RIL (2001) Chemical properties of catechols and their molecular modes of toxic action in cells, from microorganisms to mammals. Minireview. Environ Microbiol 3(2):81–91

23. Tobar N, Villar V, Santibanez JF (2010) ROS-NFκ**B** mediates TGF-β1-induced expression of urokinase-type plasminogen activator, matrix metalloproteinase-9 and cell invasion. Mol Cell Biochem 340(1–2):195–202

24. Cannito S, Novo E, di Bonzo LV, Busletta C, Colombatto S, Parola M (2010) Epithelial-mesenchymal transition: from molecular mechanisms, redox regulation to implications in human health and disease. Antioxid Redox Signal 12(12):1383–1430

25. Brunetti C, Di Ferdinando M, Fini A, Pollastri S, Tattini M (2013) Flavonoids as antioxidants and developmental regulators: relative significance in plants and humans. Int J Mol Sci 14(2):3540–3555

26. Muthuramalingam K, Cho M, Kim Y (2019) Cellular senescence and EMT crosstalk in bleomycin-induced pathogenesis of pulmonary fibrosis—an in vitro analysis. Cell Biol Int 44(2):477–487

27. dos Tenório MCS, Graciliano NG, Moura FA, de Oliveira ACM, Goulart MOF (2021) N-acetylcysteine (NAC): impacts on human health. Antioxidants 10(6):967

28. Fen F, Zhang J, Wang Z, Wu Q, Zhou X (2019) Efficacy and safety of N-acetyl-cysteine therapy for idiopathic pulmonary fibrosis: an updated systematic review and meta-analysis. Exp Ther Med. https://doi.org/10.3892/etm.2019.7579

29. Paulsen CE, Truong TH, Garcia FJ, Homann A, Gupta V, Leonard SE, Carroll KS (2011) Peroxide-dependent sulfenylation of the EGFR catalytic site enhances kinase activity. Nat Chem Biol 8(1):57–64

Publisher's Note